Journal of the Geological Society, London, Vol. **160**, 2003, pp. 719–733. Printed in Great Britain.

Effect of spatial distribution of Hormuz salt on deformation style in the Zagros fold and thrust belt: an analogue modelling approach

ABBAS BAHROUDI & HEMIN A. KOYI

Hans Ramberg Tectonic Laboratory, Department of Earth Sciences, Uppsala University, Villavägen 16, SE-752 36 Uppsala, Sweden (e-mail: Abbas.Bahroudi@geo.uu.se)

Abstract: Scaled analogue models of thin-skinned simultaneous shortening above adjacent viscous and frictional décollements simulate the effect of Hormuz salt on the shortening in the Zagros fold and thrust belt. The models consisted of sand layers that partly overlay a viscous layer of silicone and were shortened from one end. Spatial distribution of the viscous décollement varied along strike and dip, as occurs in part of the Zagros fold and thrust belt. In this belt, Phanerozoic sedimentary cover was shortened partly above the Hormuz salt lying on the Precambrian crystalline basement, behaving as a basal viscous décollement. Model results display how the nature of the décollement affects the evolution of an orogenic belt. Using model results, we explain the development of deflection zones, and discuss strain partitioning, formation of different topographic wedges and differential sedimentation along the Zagros fold and thrust belt. Model results suggest the formation of a gentle taper, consisting of both foreward and backward thrusts above a viscous décollement and a relatively steeper taper consisting only of forward-vergent imbricates above a frictional décollement. However, in our models, the steepest wedge with the highest topography formed where the viscous substrate had a limited extent with a transitional boundary (pinch-out) perpendicular to the shortening direction. Shortening of this boundary led to development of frontal ramps associated with significant uplift of the area behind the deformation front.

Keywords: Zagros fold–thrust belt, Hormuz salt, analogue modelling, thin-skinned tectonics, crustal shortening.

The basal décollement plays a significant role in controlling how fold–thrust belts deform (e.g. Davis & Engelder 1985, 1987; Butler *et al*. 1987; Velaj *et al*. 1999; Cotton & Koyi 2000; Bonini 2001). There are two end-member décollement types, viscous and frictional. Analogue and numerical modelling together with field studies show that these two end-members of décollement result in different deformation styles (Chapple 1978; Davis & Engelder 1985; Koyi 1988; Cobbold *et al*. 1989; Price & Cosgrove 1990; Dixon & Liu 1992; Liu *et al*. 1992; Talbot 1992; Letouzey *et al*. 1995; Cotton & Koyi 2000; Koyi *et al*. 2000; Costa & Vendeville 2002).

Results of mechanical tests on rock salt indicate that rock salt is very weak with high ductility at shallow levels of the crust, 3–5 km (see fig. 4 of Davis & Engelder 1987; Carter & Hansen 1983; Urai *et al*. 1986). There are more than 13 fold and thrust belts world wide that have been shortened above an evaporitic substrate acting as a viscous décollement (e.g. Davis & Engelder 1985, 1987). The presence of a viscous décollement can give rise to faster propagation of the deformation front and a lower taper in comparison with a frictional décollement during compression (e.g. Davis & Engelder 1987; Letouzey *et al*. 1995; Talbot & Alavi 1996; Cotton & Koyi 2000). However, the presence of both types of décollements within the same tectonic region results in the formation of complex structures at the boundary between the two zones (Cotton & Koyi 2000; Koyi *et al*. 2000). This variation creates differences in both the map view and the cross-section of structures (e.g. Cotton & Koyi 2000).

In this study, we use partially scaled analogue models (see the Appendix for scaling) to investigate the effect of spatial distribution of the Hormuz salt on the deformation style in the Zagros fold and thrust belt. We explain variations in structural styles between different parts of the model in plan view and cross-sections and compare them with different parts of the Zagros fold and thrust belt, and comment on changes in fold style and faulting in the cover units of the belt.

Geology of the Zagros fold and thrust belt

The Zagros mountains extend within the Alpine–Himalayean orogenic chain, for 2000 km between the central Iran plateau in the north, the Taurus in Turkey to the NW (Scott 1981), the Oman Fault in the SE (Falcon 1967; Stöcklin 1968*b*; Haynes & McQuillan 1974; Jackson & McKenzie 1984; Beydoun 1991; Beydoun *et al*. 1992; Talbot & Alavi 1996) and the Persian Gulf foreland to the SW. The Zagros fold and thrust belt has resulted from the closure of the Neo-Tethys ocean owing to convergence between the Arabian and Iranian plates, which sutured during the late Cretaceous (Sengör & Kidd 1979; Berberian & King 1981; Stoneley 1981; Snyder & Barazangi 1986; Beydoun *et al*. 1992; Berberian 1995; Talbot & Alavi 1996).

Geophysical and geological data indicate that the Zagros fold and thrust belt is currently active and is being shortened at a rate of 20–30 mm a^{-1} (Vita Finzi 1978, 2001; Jackson & McKenzie 1984; Berberian 1995; Jackson *et al*. 1995). However, recent Global Positioning System (GPS) measurements (Hessami 2002) show that the Zagros fold and thrust belt is being shortened at a lower rate (9–11 mm a^{-1}). Earthquakes of 5.5–6 M_b are common in the *c*. 200–300 km wide zone along the Zagros fold and thrust belt (Jackson 1980; Baker *et al*. 1993; Berberian 1995). This seismic activity is confined to a depth of $<$40 km (Jackson 1980; Jackson *et al*. 1981). Earthquakes in the Zagros are not precisely located by teleseismic data (Jackson & Fitch 1981; Ni & Barazangi 1986; Baker *et al*. 1993; Berberian 1995) but most of them have hypocentres located at depths of *c*. 10–20 km.

Focal-plane solutions indicate reverse faults with dips of 30–60° striking NW (Jackson 1980; Jackson *et al*. 1981; Jackson & McKenzie 1984; Ni & Barazangi 1986; Berberian 1995).

The Zagros fold and thrust belt is divided into three tectonic units across its width: the Zagros Imbricate Zone, the Zagros Simply Folded Belt and the Zagros Foredeep (Fig. 1; Stöcklin 1968b; Falcon 1967, 1974; Haynes & McQuillan 1974; Berberian erberian 1995). The boundary between the Simply Folded Belt and the Foredeep is characterized by the Mountain Front Fault, which is a structural high showing an irregular pattern in map view (Fig. 1; Berberian 1995). The Mountain Front Fault zone forms a distinct topographic step (in cross-section) where seismicity in the Zagros belt is concentrated. The fault trends NW–SE, parallel to the general trend of the Zagros belt, and delimits the distribution of linear, tight and asymmetric folds to the south. The Mountain Front Fault is proposed as a significant reactivated basement fault showing a pure dip-slip movement. This movement has led to several hundred metres of uplift in the northern part (hanging wall) and subsidence in the southern part (footwall) (see, e.g. Motiei 1993; Berberian 1995).

On the basis of litho-facies in cover sequences and the structural style along the belt, the Zagros fold and thrust belt is divided into several domains; the Lorestan domain, the Izeh domain, the Dezful embayment, the Fars Platform, the Mangrak–Kazerun domain and the Laristan domain (Fig. 1; e.g. Motiei 1995; Talbot & Alavi 1996).

The sedimentary cover (10–14 km thick) of the Zagros contains several evaporitic units with temporal and spatial variations. Among these units, the Neo-Proterozoic Hormuz salt overlying the crystalline basement is the most important unit and has controlled the deformation style of the southeastern Zagros (Fig. 2; see Talbot & Alavi 1996). As there is no complete exposure of stratigraphic sequence of Hormuz salt within the belt, its initial composition, thickness and geographical extension are estimated from the distribution of numerous extruding salt diapirs.

More than 200 salt structures of the Hormuz series have been recognized in the northeastern Arabian platform (Kent 1979; Jackson & Talbot 1986; Edgell 1996; Talbot & Alavi 1996). The distribution of emergent and buried salt diapirs shows that most of the extruded diapirs are located within three domains (the Izeh, Kazerun–Mangarak and Laristan domains) in the Zagros Simply Folded Belt (Figs 1 and 2). Husseini (1988) attributed the 'irregular' distribution of Hormuz salt to Late Precambrian faults. The experiments described in the next section were designed to investigate the conditions that may have controlled the structural pattern in the Zagros fold and thrust belt.

Model preparation

Two models were prepared in this study. Each consisted of layered sand simulating the sedimentary overburden in the Zagros fold and thrust belt, resting on a viscous substrate that had a geographically uneven distribution. The distribution of the viscous layer, which simulated Hormuz salt, was such that in some parts of the models, the sand layer was resting directly on the rigid substrate (Fig. 3). In our model, we have simplified the distribution pattern of Hormuz salt, so that the boundary between frictional and viscous décollements separating different domains is parallel to the shortening direction. This distribution divided the model into five domains labelled A to E to compare with their prototypes in the Zagros fold and thrust belt (see below). The base of each model was horizontal and flat. The models thus contained areas underlain by frictional or viscous décollements above which the sand overburden was shortened.

Loose sand has often been used to simulate a frictional cover

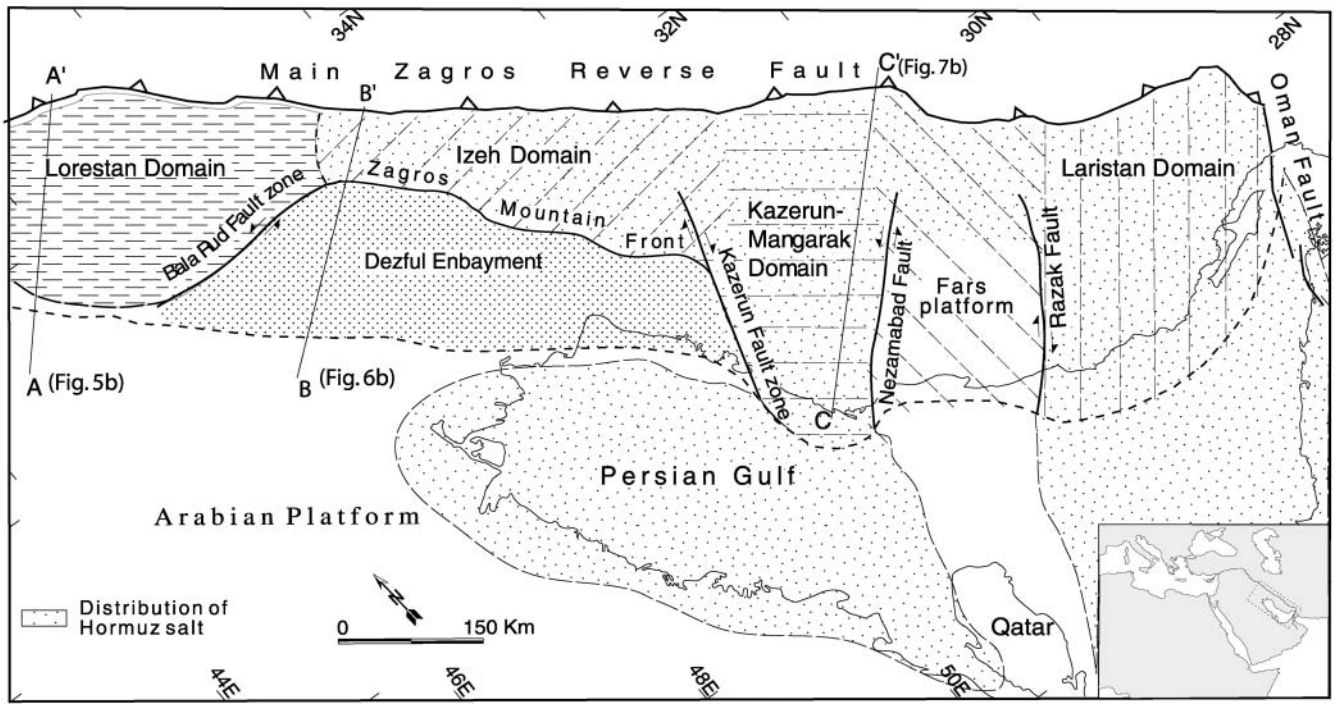

Fig. 1. Distribution of the Hormuz salt and major structural domains (the Laristan domain, the Fars platform, the Kazerun–Mangarak, Izeh and Lorestan domains, and the Dezful embayment) and main faults (the Razak, Nezamabad, Kazerun and Bala Rud faults) along the Zagros belt.

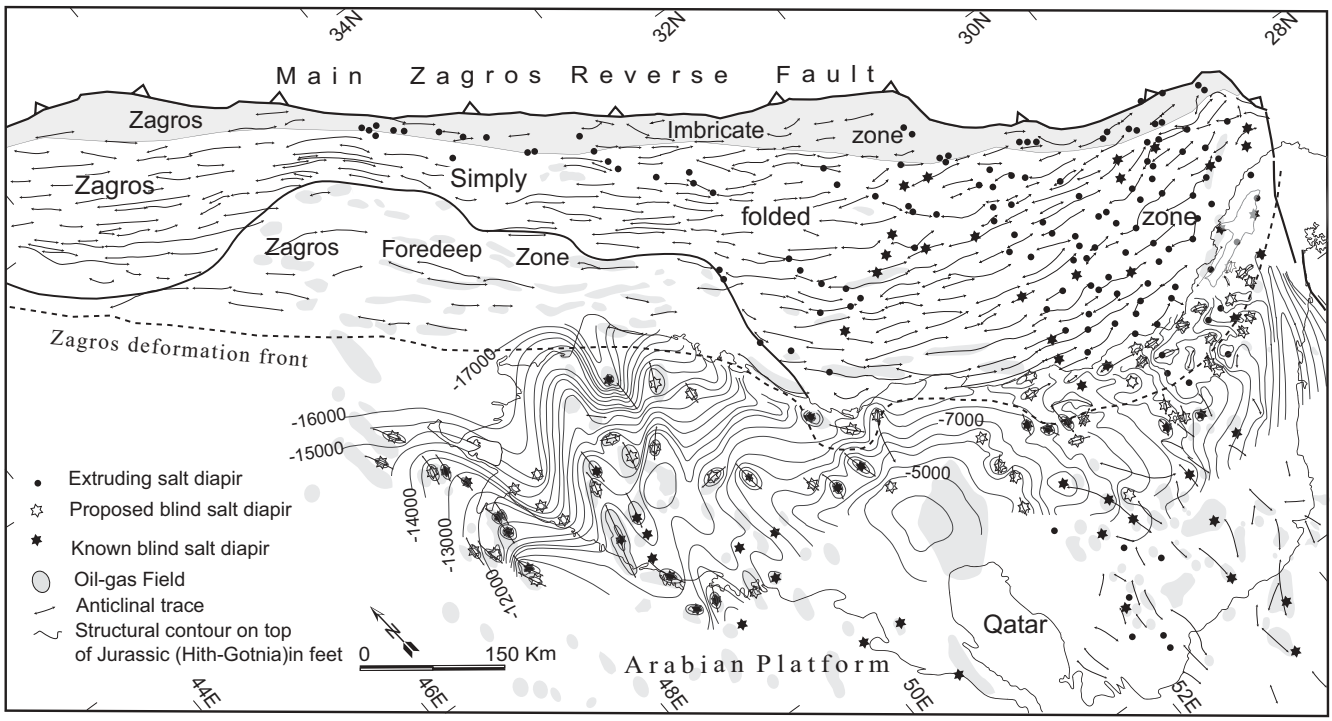

Fig. 2. Distribution of major structural units including the Zagros Imbricate Zone, the Zagros Simply Folded Zone and the Zagros Foredeep across the Zagros fold and thrust belt, including anticlines, salt structures of the Hormuz series, and hydrocarbon reserves in the belt and its foreland basin. In this map structural contours on uppermost Jurassic (Hith–Gotnia anhydrite) show the main structural trends in the Persian Gulf. The Zagros deformation front separates two regions with different structural trends, NW–SE and north–south, shown by hydrocarbon fields and folds.

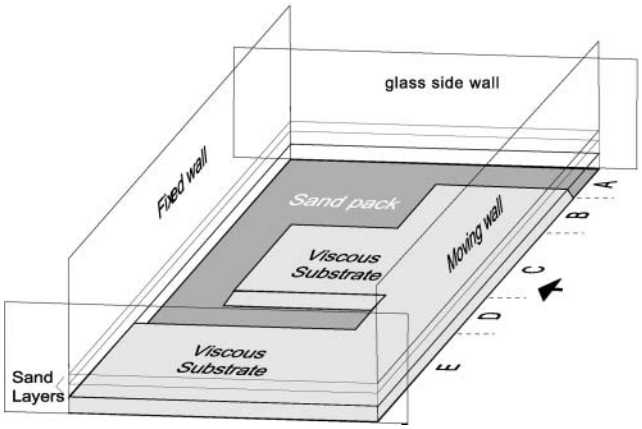

Fig. 3. Schematic illustration of initial configuration of the ductile (SGM-36) and brittle (sand) décollements in the models, showing the shortening direction and domains A–E.

(Davy & Cobbold 1991; Weijermars *et al*. 1993; Cotton & Koyi 2000; Bonini 2001; Costa & Vendeville 2002). The bulk density ρ of the sand used in the models was 1700 kg m^{-3} with a cohesive strength C of 140 Pa and an average grain size of about $\geqslant$35 μm (Cotton & Koyi 2000). The Newtonian viscous material SGM-36, which is manufactured by Dow Corning Ltd, has density of 987 kg m^{-3} with effective viscosity η of 5×10^4 Pa s at room temperature (*c*. 20 °C). SGM-36 has been used in past studies to simulate, for example, evaporitic deposits or over-pressured shale (Weijermars *et al*. 1993; Letouzey *et al*. 1995; Cotton & Koyi 2000; Bonini 2001; Costa & Vendeville 2002).

The models were prepared in a deformation rig with initial dimensions 60 × 50 cm on an aluminium-topped table representing a rigid basement (Fig. 3). Initial thicknesses of the viscous substrate and the overlying cover were 0.5 cm and 1.5 cm, respectively. The total thickness of the models was 2 cm. Compression was applied at a uniform rate of 1.15 cm h^{-1} (3.2×10^{-4} m s^{-1}) from one end using a motor-driven worm screw. The models were shortened by up to 30% during 15.6 h.

A grid of marker squares (1.2 cm × 1.2 cm) was printed on the top surface of the models, which was photographed at fixed time intervals to record surficial structures formed during deformation. After the desired bulk shortening, the deformed models were covered by loose sand and impregnated by water. This process saturated the sand layers and increased their cohesive strength, thus allowing vertical cross-sections to be cut for photography.

Model kinematics and results

During shortening, both overburden layer and the viscous substrate were deformed. The sand cover deformed differently above the frictional and viscous décollements. Below, we describe deformation of different domains (A–E; Fig. 4) of the models in plan view and in cross-sections. For each domain, description of its deformation (from map view and different profiles) will be followed by description of deformation in the natural prototype they simulate. We define the 'width' of a domain as the distance along the dip, whereas the 'length' of a domain is that along strike.

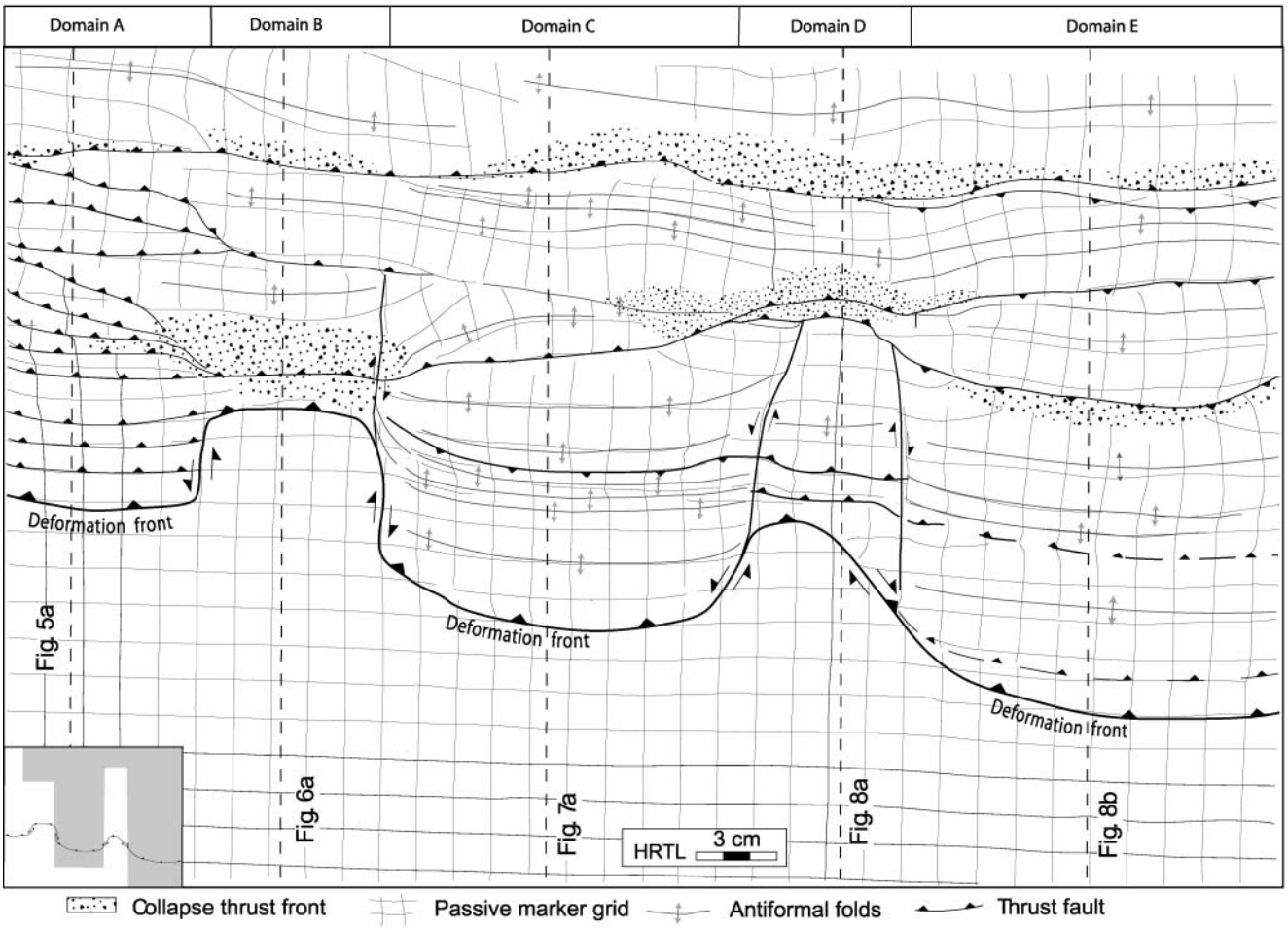

Fig. 4. Top view of the model after 30% of bulk shortening, showing formation of different deflection zones across the deformation front propagating above the viscous and frictional substrates. It should be noted that differential propagation of the deformation front in the various domains of the model resulted in variation in structural style. The inset is a top view showing the initial distribution of the viscous layer (grey area) and the deformation front at 30% bulk shortening.

Domain A

The first compressional structures appeared above the frictional décollement in domain A where the cover sand layer rested on a rigid base (Fig. 3). Shortening led to formation of a piggyback stack of imbricate thrusts. The square markers initially printed on the surface of the model showed compression perpendicular to the strike of the thrusts during the deformation. Laterally, the thrust faults in this domain merged toward domain B as lateral ramps (Fig. 4).

The width of the deformation zone in this domain reached 19 cm after 30% of bulk shortening (Figs 4 and 5). This width was larger than that in domain B, where the deformation front had not propagated as far (see below). This difference in width between domains A and B is manifested in deflection of the deformation front (Fig. 4). The deflection in deformation front that is due to a change from a frictional décollement in domain A to viscous décollement in domain B (Fig. 3) is accommodated by a left-lateral strike-slip fault. This fault offsets the deformation front about 4 cm (Fig. 4).

In cross-section, the thrust faults dip towards the hinterland and are closely spaced. The initial dip of each new thrust fault was *c*. 23° (Fig. 5a). The dip increased as a result of back-rotation of the imbricates as new thrust faults formed in front of older ones. This process also led to deformation of the fault planes. The wedge taper was steep (19°) (Fig. 5a).

Compression within the Lorestan domain

Domain A of the model can be compared with the Lorestan domain, where Hormuz salt is absent (Fig. 1). This area consists of many closely spaced thrust faults and fault-related folds (Figs 2 and 6).

In map view, the traces of folds and thrust faults are linear and extend for 87 km on average. The wedge in this domain has a high taper and a constant topographic dip along the belt (see fig. 3c of Talbot & Alavi 1996). Southwards the folds in this domain are delimited by the Mountain Front Fault, which separates the deformed areas in the north from the less deformed Dezful embayment (Fig. 1). The boundary between the Dezful embayment and the Lorestan domain is defined by the 'Mountain Front Flexure or bending' on map view (Falcon 1961) which coincides with the Bala Rud left-lateral fault zone (see Berberian 1995). This structural feature is comparable with the deflection formed between domains A and B in our models.

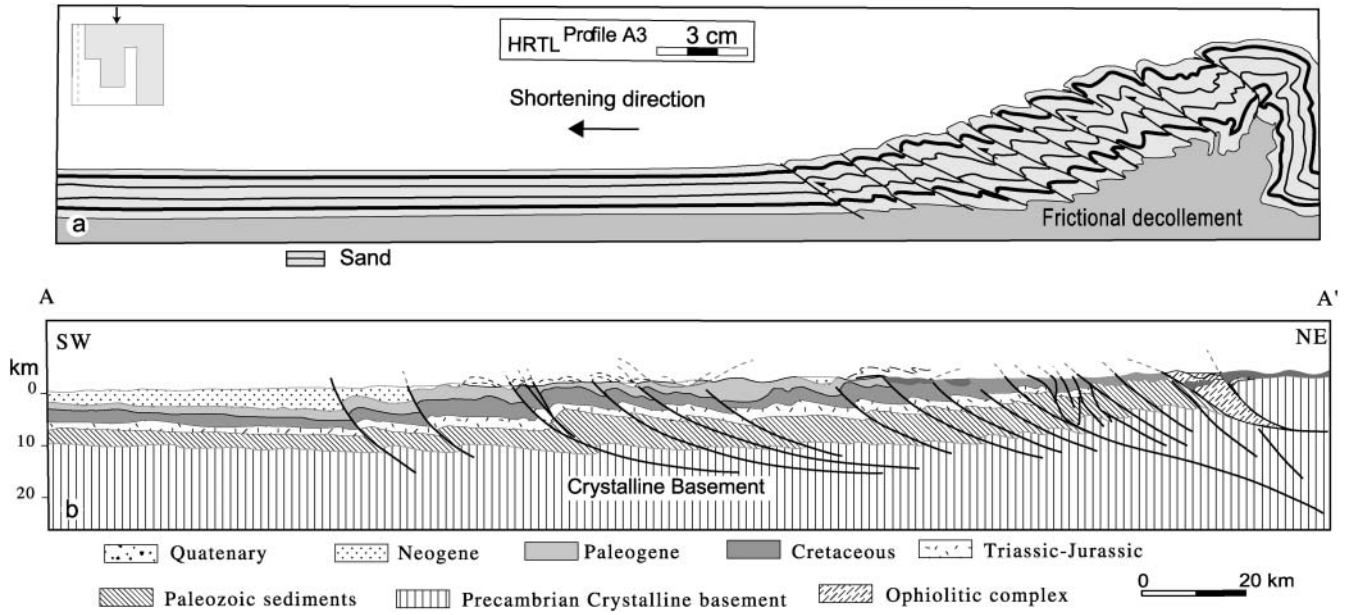

Fig. 5. (**a**) Line drawing of a profile along domain A parallel to the shortening direction (see Fig. 4 for location) showing a steep taper of an imbricate stack of closely spaced thrust faults formed above a frictional décollement (inset is a top view showing the location of the cross-section). (**b**) Geological cross-section of the Lorestan domain (see Fig. 1 for location) showing an imbricate stack in the cover and basal units (redrawn from Spaargaren 1987).

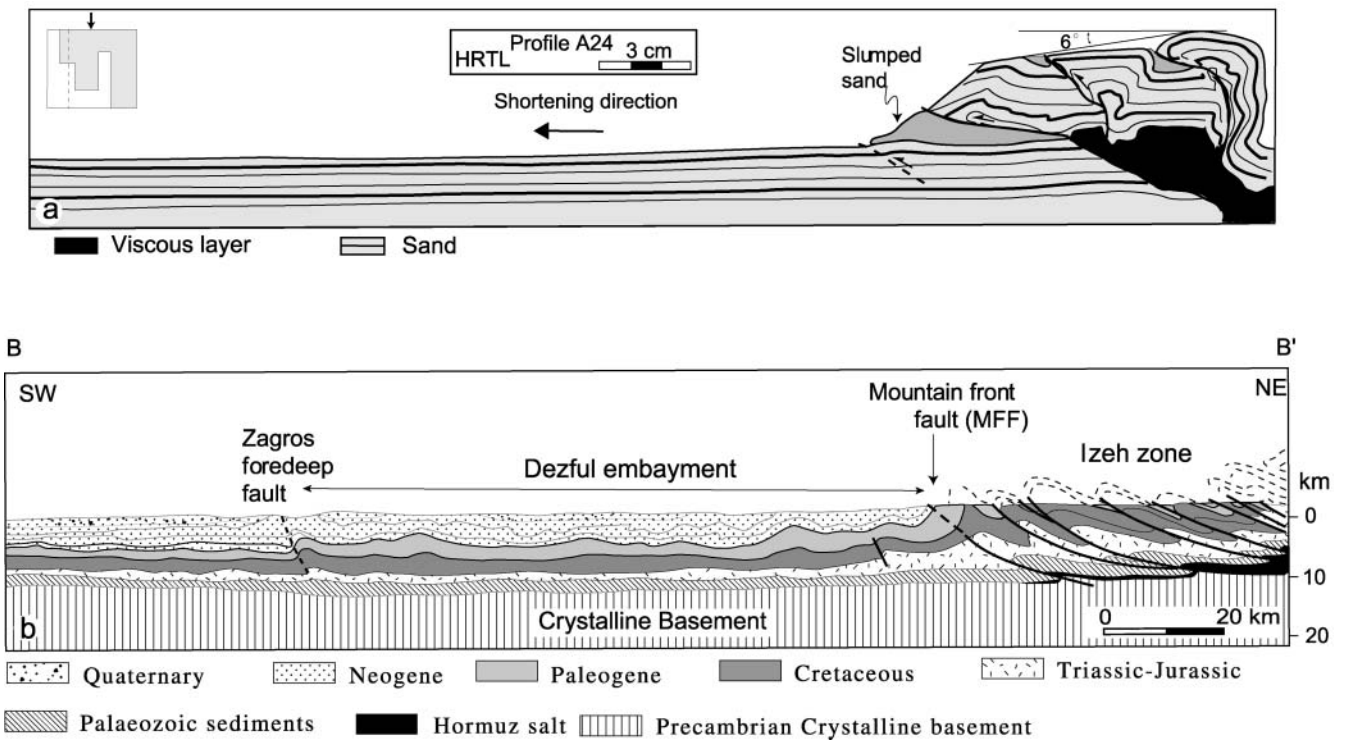

Fig. 6. (**a**) Line drawing of a profile along domain B (see Fig. 4 for location) parallel to the shortening direction, showing narrow taper with some thrust faults above the viscous substrate, which abruptly changes into a frictional substrate. The pronounced thickening of the viscous material against the footwall ramp at the boundary between the viscous and frictional décollements should be noted. In this part of the model, slumped sand was run over by the hanging wall of the frontal fault (inset is a top view showing the location of the cross-section). (**b**) Geological cross-section of the Izeh domain and the Dezful embayment across the Zagros belt (see Fig. 1 for location) showing a narrow imbricate stack formed behind the Mountain Front Fault, which separates the Dezful embayment, with low deformation, from the highly deformed Izeh domain (redrawn from Spaargaren 1987).

The geological cross-section of the Lorestan domain shows a sequence of foreland-verging, NE-dipping thrust faults, associated with NW–SE-trending folds (Fig. 5b). These structures form a piggyback imbricate stack. The structures shown in this cross-section are similar in geometry to those developed in domain A of the model (compare Figs 5 and 6). The geological cross-section of this area (Fig. 5b) shows a one-to-one structural relationship (Spaargaren 1987) between the basement and cover, indicating coupled deformation between the two units. We do not share the interpretation of that cross-section in Figure 6. Instead, we suggest that even though deformation is thick skinned in the Zagros, deformation in the cover was very probably decoupled in many places from the basement, and we therefore compare our model results only with the deformation in the cover units.

Domain B

Domain B is the shortest deformed zone (14 cm) in plan view (Fig. 4). In this domain, part of the sand layers rested on a viscous layer. This domain was bounded laterally on both sides by deflection of the deformation front associated with strike-slip deformation. The topography of domain B is relatively high and abrupt compared with that of other domains (Fig. 6a). The deformation front in this domain coincides with a very significant topographic step of 3 cm in elevation. Nevertheless, the top surface of the whole deformed area shows relatively gentle slope of about 6° (Fig. 6a).

The square markers in this domain underwent shortening in the beginning. However, with progressive deformation, markers above anticlinal crests were extended in the shortening direction (Fig. 4).

Although the amount of bulk shortening is the same in these two domains, the total number of faults decreases from domain A (17) to domain B (four) (Figs 4 and 7). Therefore, individually, the fewer faults in domain B show larger displacement compared with those formed in domain A.

In cross-section, the viscous layer is thickened behind a frontal ramp at the boundary between frictional and viscous domains (Fig. 6a). This pre-existing ramp had a 25° dip, and mimics the SW extent of Hormuz salt in this domain. During shortening, sand layers resting above the viscous substrate were mostly shortened and carried up by the frontal thrust fault along the ramp (Fig. 6a). The viscous material is smeared and passively carried upward along the thrust faults. Slip along the frontal thrust is high, about 8 cm. This large displacement led to a local thickening of the viscous layer in domain B to more than twice its initial thickness. This frontal thrust fault formed at an early stage (about 5% of shortening) of the deformation. No faults formed in front of this thrust even at 25% of shortening.

The Izeh domain

Domain B can be compared with the Izeh domain located NE of the Dezful embayment (Figs 1, 4 and 8), where exposure of salt structures along fault zones implies the presence of the Hormuz series at the base of the sedimentary cover (Fig. 6b). This domain is separated from the Dezful embayment by the Mountain Front Fault and it differs from the Lorestan domain to the NW by a change in deformation style (e.g. Falcon 1961; Berberian & Tchalenko 1976; Berberian 1995). The Izeh domain extends for about 350 km in length and 100 km in width. This domain consists of long fault-propagated folds (86.7 km long on average

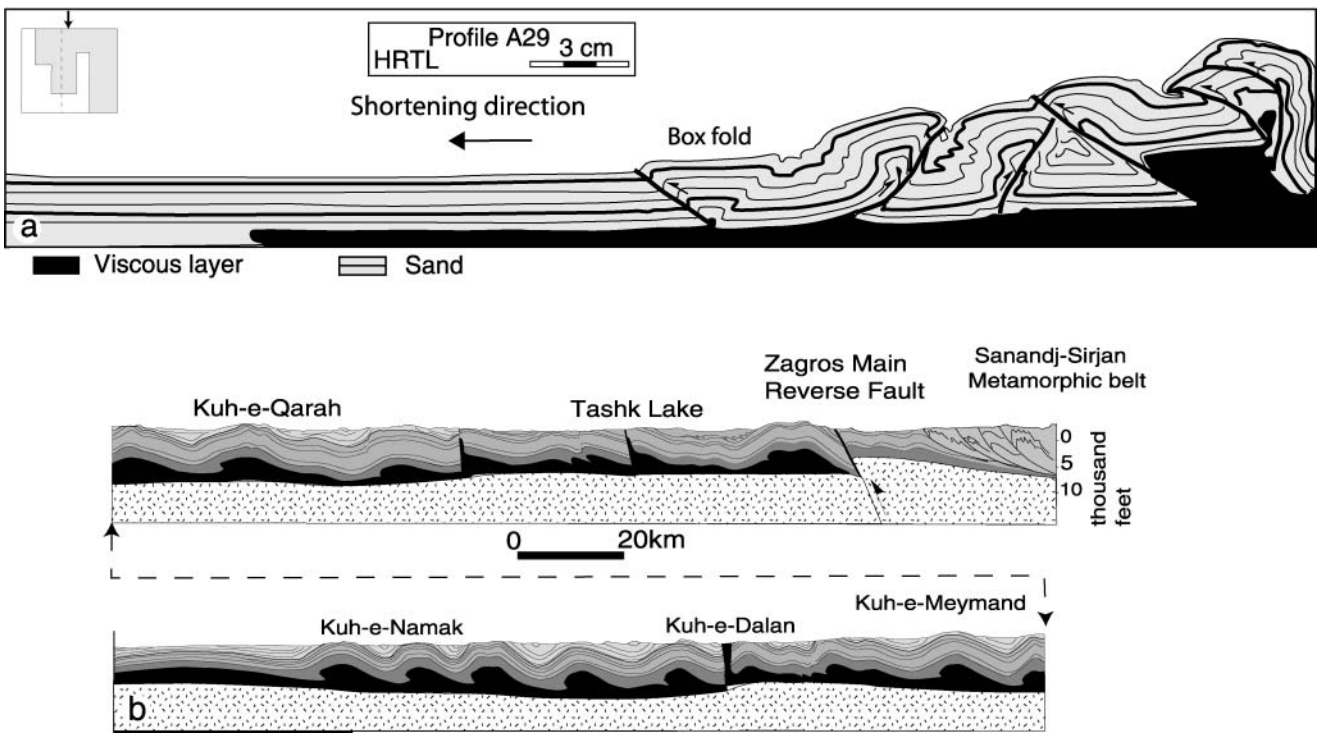

Fig. 7. (**a**) Line drawing of a profile along domain C (see Fig. 4 for location) parallel to shortening direction showing a low-angle, wide taper with thrust faults including fore- and back-thrusts and fault-related folds above the viscous substrate. The pronounced thickening of the ductile substrate, partly forward flow and its injection along some of the fault planes should be noted. (Inset is a top view showing location of the cross-section.). (**b**) Geological cross-section of the Laristan domain across the southeastern Zagros belt (see Fig. 1 for location) showing a wide folded zone consisting of the salt-cored anticlines (redrawn from National Iranian Oil Company 1975).

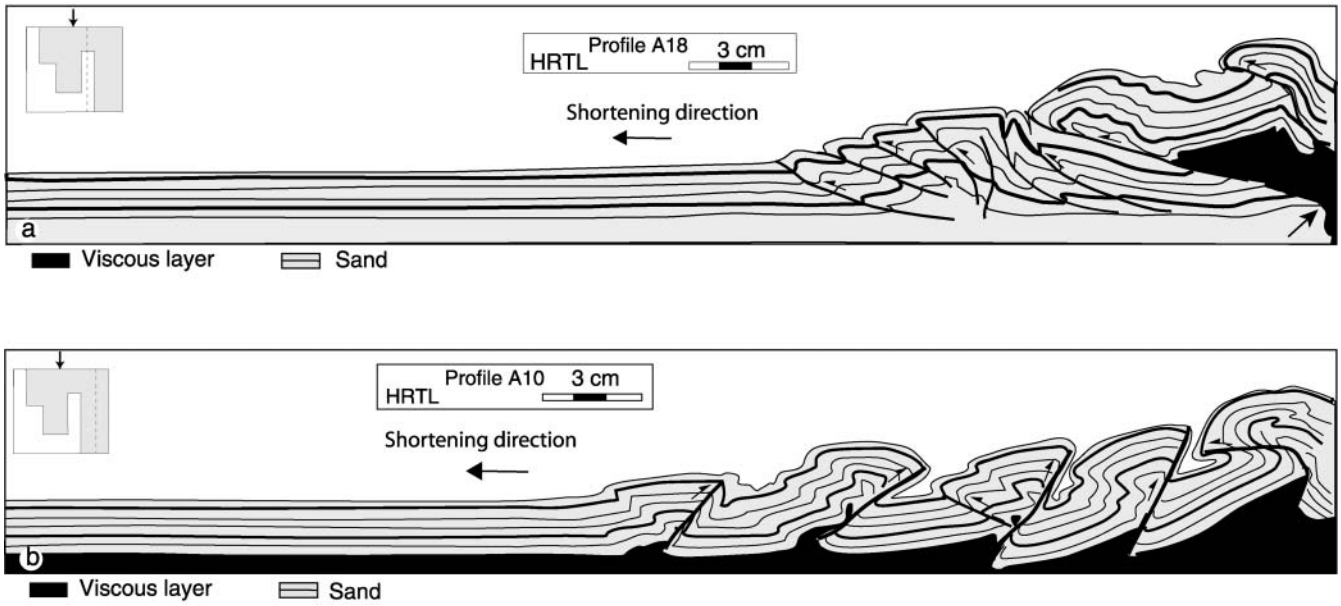

Fig. 8. (**a**) Line drawing of a profile along domain D (see Fig. 4 for location) parallel to the shortening direction, showing an irregular taper with two topographic slopes. Above the ductile substrate, a few fore-thrust faults propagated forward and ramped over the frontal boundary B between the ductile and frictional substrates (thick arrow). Deformation is accommodated above the frictional décollement by formation of many more fore-thrusts verging towards the foreland. The thickening of the ductile substrate should be noted. (**b**) Line drawing of a profile along domain E (see Fig. 4 for location) parallel to the shortening direction, showing a wide and low taper with thrust faults, mainly back-thrusts, few fore-thrusts and fault-related folds above ductile substrate. In this profile, anticlines were superposed on top of synclines bounded by fore- and back-thrust formed pop-down structures, which sank into the viscous layer and restricted the forward migration. The pronounced thickening of the ductile substrate beneath the anticlines and its injection along the planes of the back-thrusts should be noted. (Inset is a top view showing the location of the cross-section.)

but in some cases up to 200–310 km long). In cross-section, these southward-verging asymmetric and tight folds are 7.3 km wide and 2–3 km high.

The Mountain Front Fault is the most important topographic and morphological feature of the Zagros fold and thrust belt, with structural and seismic characteristics. Fault-plane solutions of earthquakes along the Mountain Front Fault indicate pure dip-slip thrust faulting (Berberian 1995). Based on stratigraphic, seismic and borehole data, the vertical displacement along the Mountain Front Fault is estimated to be 3–6 km (Berberian 1995; Motiei 1995). This high topography was subjected to a significant amount of erosion, which provided the detrital materials that were deposited in the subsiding Dezful embayment in the Neogene (Fig. 2).

Domain C

In plan view, the width of this deformation zone increases remarkably from domain B into domain C (about 23 cm). This domain was floored entirely by a viscous décollement (Fig. 4). The boundary between domains B and C was characterized by the deflection in a deformation front, which formed a lateral ramp. Here, the deformation front was offset about 5 cm along a right-lateral strike-slip zone. The deformation front in this domain has propagated further away from the moving wall compared with domain B. Shortening resulted in the development of more folds and faults in this domain compared with domain B. The spacing of these structures was generally longer than in domains A and B (Fig. 6b).

The square markers on top of the model continuously underwent a complicated strain path from compression to extension during deformation. This complicated strain path can be attributed to internal deformation of each thrust sheet during progressive shortening. At the onset of deformation, the thrust sheets underwent compression, shown by the shortened markers. However, as the thrust sheets grow, the outer area of their anticlinal crest is extended. It has been previously reported that because of extension of the outer arc of such anticlines, graben form above their crests (e.g. Cotton & Koyi 2000).

In cross-section, domain C displays a topographic slope (*c.* 10°) gentler than that in other domains. The section shows thrust faults and fault-related folds (Fig. 7a). In contrast to domain A, where shortening resulted in only forward-verging faults, in domain C, both fore- and back-thrusts formed (Fig. 7a).

Above the viscous substrate, box folds are common. The fore- or back-limbs of these folds were overturned later and subsequently displaced by either the fore- or back-thrusts (Fig. 7a). Different cross-sections in domain C show that, although there was no dominant preferred vergence for the thrust faults, the back-thrusts were relatively more abundant.

The Mangarak–Kazerun domain

We compare domain C with the Mangarak–Kazerun domain, where many extruding salt structures indicate that the Hormuz salt was present throughout this domain (e.g. Kent 1958, 1979; Talbot & Alavi 1996). Distribution of emergent and buried salt structures indicates that the Hormuz salt extends further SW into the Persian Gulf and Arabia (Fig. 7b).

The width of the deformation zone of the Zagros fold and thrust belt increases in this part and reaches 350 km (Talbot & Alavi 1996). The north–south-trending, 300–450 km long Kazerun Fault forms the boundary between this zone and the Dezful embayment to the west (see Fig. 1; Kent 1958, 1979; Falcon

1967, 1974; Baker *et al*. 1993; Berberian 1995; Talbot & Alavi 1996; Sepehr 2001). The Kazerun Fault intersects, offsets and bends the NW–SE-trending folded structures of the Zagros. This fault is proposed to be a reactivated north–south-trending basement fault (Falcon 1961, 1974; Berberian 1995; Motiei 1995; Sepehr 2001) and is divided into segments on the basis of geometry, age and displacement (e.g. Berberian 1995;Sepehr 2001). Earthquake focal mechanism solutions, and structural and morphological characteristics show a right-lateral strike-slip movement along this fault (e.g. Baker *et al*. 1993; Berberian 1995; Sepehr 2001). The net amount of displacement along the Kazerun Fault has been estimated to be 150 km using the offset of the Mountain Front Fault between the western and eastern sides of the fault (Berberian 1995).

Domain D

Domain D acts as a narrow and resistant buttress, and is characterized by a steeper topographic slope than surrounding domains, C and E. In this domain, the width of the domain reduced from 24 cm in domain C to 17 cm after 30% of bulk shortening. Lateral boundaries of this domain are characterized by two deflection zones. The deformation front was offset left-laterally by about 4 cm between domains C and D.

In cross-section, domain D shows a stepwise morphology formed by the former position of the deformation front above the viscous–frictional décollement boundary and the current position of the front (Fig. 8a).

Cross-sections cut along domain D show two different styles of deformation (Fig. 8a). Above the viscous décollement, the layers were thickened to almost three times their initial thickness after 30% of bulk shortening. At this stage the backstop had almost passed beyond the initial frontal viscous–frictional boundary and detached the viscous substrate from the rigid base to form a thickened wedge within the overburden (Fig. 8a). Here, the thrust that overrides the frontal ramp showed a large displacement before formation of the current frontal fault. This feature was very similar to that in domain B (compare Fig. 6a with Fig. 8a). This part consisted of a fault-related fold with larger (about 5 cm) spacing.

Deformation above the frictional part of this domain resulted in closely spaced foreland verging thrust faults. These structures were similar in geometry to those in domain A.

The Fars domain

The Fars domain, which we defined as the area between the Nezamabad and Razak faults, extends as a long and narrow strip nearly perpendicular to the general trend of the Main Zagros Reverse Fault (Fig. 1). Folds in the Fars domain between the Kazerun–Mangarak domain (see Kent 1979; Talbot & Alavi 1996) and the Laristan domain are straight and long; some are 128 km long and 9.5 km wide. The absence of salt structures, whether emergent or buried, implies that the Hormuz salt was either never deposited or is very thin on the Fars platform. This assumption is not conclusive, as the absence of salt structures in the SW part of this domain (the Fars platform) may also depend on the lack of adequate triggering mechanisms. However, it is rather puzzling that only in this part of the SE zones such triggering mechanisms did not operate.

The deformation front is bounded by two deflection zones at boundaries between the Mangarak–Kazerun domain to the NW and Laristan domain to the SE. These boundaries are represented by NE–SW-trending strike-slip faults, the Nezamabad Fault to the west and the Razak Fault to the east (Fig. 1; Barzegar 1994; Motiei 1995). The Nezamabad Fault is about 265 km long and shows a left-lateral sense of movement (Motiei 1995). The Razak Fault, which extends about 230 km along the eastern boundary of the Fars platform, is a right-lateral fault (Barzegar 1994). To the NE, the platform is delimited by thrust faults of the Zagros Imbricate Zone.

Domain E

In this part of the model, the viscous layer extended over the entire length of the model. During shortening, the deformation front propagated further away from the backstop, developing a gentle taper of about 7°, similar to that in domain C (Fig. 8b). In domain E, the second syntaxial zone, 25 cm wide, was formed in the model (Fig. 4). The overburden sand layers were deformed by thrust-bounded folds. Anticlinal folds were cored by very thin volumes of the viscous material. There were also thin smears of the viscous material along some of the fault planes. The viscous substrate was thickened mainly beneath the deformation zone; being thickest close to the backstop. The trend of these structures changed across domain E. Spacing of the structures was larger than that in domains A, B and D. Domain E, which was structurally similar to domain C, was confined laterally by a large deflection formed at the contact with domain D.

The Laristan domain

In the extreme SE of the Zagros fold and thrust belt, the Laristan domain is characterized structurally by the presence of many salt structures that penetrated the sedimentary cover. This area is delimited laterally by the Fars platform to the NW and the Oman line toward the SE (Fig. 1). The width of this domain reaches 350 km (Talbot & Alavi 1996). In the Laristan domain, the main structural features are gently dipping double-plunging folds with sinusoidal traces on map view. These folds are 41.7 km long on average and about 10 km wide in cross-section. In the north of the area towards the Main Zagros Reverse Fault, thrusts are dominant. The Oman Fault separates the Zagros fold and thrust belt from the Makran accretionary wedge in the east. Topographic profiles across the Laristan domain show a low gradient, which is confirmed by a gentle taper of $\leqslant 1°$ (Talbot & Alavi 1996).

Discussion

The two main goals in this study were to (1) show the role of Hormuz salt in the style of deformation during the Zagros orogeny, and (2) better understand post-Cretaceous sedimentary facies changes. Model results presented here show a general match between the model and its prototype, the Zagros fold and thrust belt (see Appendix). Below, we will analyse and compare some of the main results of the models with geological evidence from the Zagros fold and thrust belt.

Geometry of the deformation front

Variation in deformation style in the models, which was controlled by spatial distribution of the viscous substrate simulating rock salt, was visible both in plan view and in cross-section. In plan view, bending in the deformation front clearly reflected differential propagation of deformation as a result of variation in basal décollement (Fig. 4). Above the viscous décollement, the front propagated faster and further than above the frictional

décollement. This led to a change in width of the deformation zone in different parts of the model; the deformation zone is wider above the viscous décollement (e.g. domain C and partly domain D). By contrast, the width of the deformation zone is less above the frictional décollement (compare domain A with domain C or D). This difference in the width of the deformation zone has been reported by previous workers (e.g. Davis & Engelder 1985, 1987; Marshak *et al*. 1992; Cotton & Koyi 2000; Costa & Vendeville 2002). However, in this study, the viscous substrate changed not only along strike, but also across it. This led to a significant change in style of deformation, for example in domains B and D, where the deformation zone was shorter even though these two domains were floored partly by a viscous layer. In domains B and D, where the viscous décollement changed to a frictional one perpendicular to the shortening direction (see Fig. 3), the width of the deformation zone is less than in domain A, which is entirely shortened above a frictional décollement. Both the cover and décollement were shortened and thickened in these domains. However, the presence of the viscous décollement in domains B and D led to easier and more intensive deformation of the overlying cover than that above the frictional décollement. This resulted in accommodation of larger deformation against the frontal ramp, where a large amount of displacement took place. As a result, the overburden units were shortened more above the thickened viscous layer, and the deformation front did not propagate as far as in domains C and E, which were floored entirely by a viscous layer.

In the Zagros fold and thrust belt, distribution of the Hormuz salt also changes both parallel and perpendicular to the general direction of the regional shortening (Fig. 1). North of the Dezful embayment (simulated by domain B in the model) the boundary between the viscous and frictional décollements is roughly perpendicular to the NE shortening. This has led to development of a significant morphotectonic feature, the Mountain Front Fault, which separates the Izeh zone, which has intense deformation, from the Dezful embayment with significantly less deformation (Figs 1 and 8).

Sand models with variable thickness along strike shortened from one end show that the deformation front propagates further in the domains with thicker units than in the domains with thinner units (Marshak *et al*. 1992). It is possible that initial thickness variation along the Zagros fold and thrust belt may have played a role in the formation of an offset deformation front. However, thickness variation along the Zagros fold and thrust belt is not entirely consistent with the zone of offset of the deformation front. The sedimentary thickness in the northwestern part of the Dezful embayment, where Hormuz salt is missing, is *c*. 14 km compared with 10–12 km in the Fars and Kazerun–Mangerak domains, where Hormuz salt is present (Motiei 1995). However, the deformation front in these two domains has propagated further than in the Dezful embayment. Therefore we suggest that even though the sedimentary thickness variation may have played some role in differential propagation of the deformation front, the effect of the Hormuz salt décollement must have been more significant.

It has been suggested that the Mountain Front Fault is a reactivated basement fault (e.g. Falcon 1961, 1974; Berberian 1995; Motiei 1995). However, model results imply that even in the absence of any reactivated faults in the basement, the irregular distribution of Hormuz salt, during the post-Cretaceous shortening, can lead to development of a structural feature that is very similar to the Mountain Front Fault.

Some workers (Ricou *et al*. 1977; Berberian 1995) have used different terms to distinguish the Mountain Front Fault from the deformation front in the Zagros fold and thrust belt. The deformation front separates the undeformed sequence to the SW on the Arabian platform from the deformed sequence to the NE, whereas the Mountain Front Fault appears to separate the highly deformed areas from less deformed regions within the Zagros belt (see Berberian 1995). The two fronts are located near each other (0–50 km apart) in the Lorestan, the Mangarak–Kazerun and the Laristan domains (Fig. 1). However, in the Dezful embayment, the Mountain Front Fault is about 150–170 km behind the deformation front.

Talbot & Alavi (1996) defined a constant width for the Zagros belt east of the Kazerun Fault. They showed the Zagros deformation front as a continuous curvature that coincides with nearly the 50 fathom water-depth contour and the shape of oil and gas fields (see fig. 3 of Talbot & Alavi 1996). They pointed out that north–south-trending oil–gas fields on the Arabian platform were deformed to NW–SE Zagros trends behind the front. The deformation front is defined where those fields show an intermediate shape (Talbot & Alavi 1996). It is important to underline that the NW–SE orientation of the oil fields may be primary Zagros trends in previously undeformed younger units not affected by the Arabian trend. However, to prepare a good estimation and determine a more detailed geometry of the deformation front we use the change in shape of oil–gas fields and integrate it with structures shown in the structural contour map of the Upper Jurassic anhydrite (Hith–Gothnia formation) in the Persian Gulf and onshore (Fig. 2). Our examination shows that the deformation front, east of the Kazerun Fault, is not a simple antitaxial arc, but consists of two antitaxial arcs with a syntaxial arc between them. We attribute this geometry of the deformation front to the spatial distribution of Hormuz salt in this part of the Zagros fold and thrust belt. This syntaxial arc is similar to domain D in our models.

Model results show that the geometry of the deformation front could be complicated by the non-uniform distribution of the basal viscous substrate leading to a small additional syntaxis above domain D simulating the Fars platform (Figs 2 and 4). The model results also show the presence of antitaxial–syntaxial geometry, which fits very well with that observed in the Fars platform (compare Figs 2 and 4).

Strain partitioning

Differential propagation of the deformation front was visible between the domains from the early stages of shortening (Fig. 9). This in turn led to strain partitioning and changes in deformation style in different parts of the model. In domains B and D, which were partly floored by a viscous layer, deformation propagated further at the beginning of the shortening (Fig. 9). However, with progressive shortening, the deformation front in these two domains did not propagate beyond the viscous décollement into the area underlain by the frictional décollement directly where the deformation front reached this area. The forward advance of the deformation front ceased for a considerable amount of shortening (about 20% of bulk shortening).

In domain B, the viscous substrate was displaced by the moving backstop and accumulated as a thick wedge against the frontal ramp (Fig. 6a). This process led to thickening of overburden above the viscous décollement until the viscous substrate was entirely scraped off from the base by the backstop. After that stage, the deformation occurred above the frictional décollement. The variation in décollement along the shortening direction led to the formation of a different topographic slope in domain B and to some extent in domain D where the viscous substrate

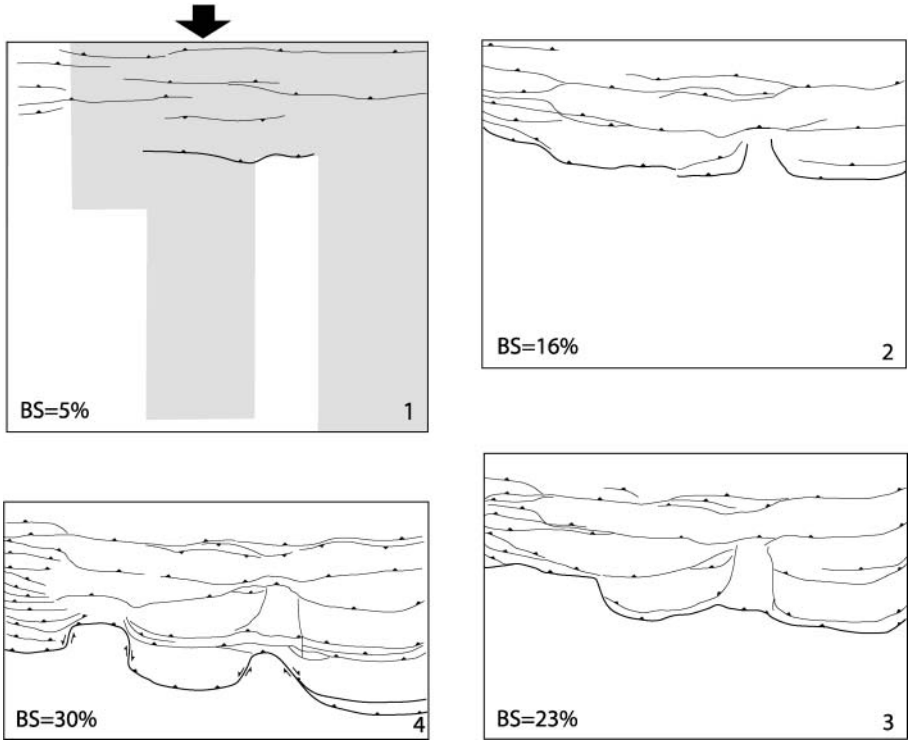

Fig. 9. Line drawing of the model at different stages of shortening, showing sequential formation of main structural features and advance of the deformation front. Grey shading in stage 1 shows the initial distribution of the viscous layer before any shortening took place. BS, bulk shortening.

successively tapered to a frictional décollement. The viscous substrate accommodated the shortening by ductile thickening whereas the overlying sand layer accommodated it by folding and imbrication (Figs 7 and 8).

Similar to the model, shortening in the Izeh domain must have been accommodated by ductile thickening of Hormuz salt and folding and imbrication of the cover units (see Fig. 6b). Sedimentary facies changes reported in the vicinity of the Mountain Front Fault indicate that the location of this fault has remained stationary since the late Eocene and its forward advance must have slowed during a considerable amount of the shortening in the Zagros fold and thrust belt. This suggests that most of the shortening must have been accommodated within the region NE of the Mountain Front Fault. This scenario is similar to our model, where most of the deformation took place behind the frontal ramp in domain B, between the viscous and frictional décollements.

Effect of differential propagation on sedimentation

The boundary between the viscous and frictional décollements in domain B was perpendicular to the shortening direction (Fig. 3). This boundary acted as a frontal ramp against which a high uplifted area formed. Although there is no major subsidence in front of this uplifted area underlain by the frictional décollement (see Figs 4 and 7), such an abrupt step across the deformation front is likely to induce subsidence in a natural example. The Dezful embayment in the Zagros fold and thrust belt is interpreted to represent such a subsidence where thick sediments have accumulated.

Based on model results, we infer that a frontal ramp (the Mountain Front Fault) in the Zagros fold and thrust belt and subsidence in the Dezful embayment (acting as a foreland) formed in the late Eocene (e.g. Berberian 1995; Motiei 1995). The Dezful embayment was a sedimentary basin with pronounced subsidence where thick late Eocene–Recent deposits were formed. The Dezful embayment formed a delta during sedimentation of the Asmari carbonates, to which a substantial amount of hydrocarbons migrated from mid-Cretaceous source rocks (James & Wynd 1965; Murris 1980; Berberian & King 1981; Beydoun *et al*. 1992; Motiei 1993, 1995). Erosion of the uplifted domains, particularly the Izeh domain to the NE, provided more sediment, whereas, on the SW side, clastic material from the Arabian shield was transported into the embayment (e.g. Motiei 1993). This process resulted in formation of the thickest sedimentary sequence of the Zagros fold and thrust belt in the Dezful embayment. More subsidence increased burial depth of the source rocks in this area. As a result, organic material matured faster here than in the other domains. This can probably explain the huge accumulation of hydrocarbons in the Dezful embayment.

The Mountain Front Fault formed at the frontal boundary between the viscous décollement (represented by Hormuz salt) to the NE of the Dezful embayment and the frictional décollement (represented by lack of Hormuz salt) to the SW of it. At least 6 km of sedimentary rocks from the Izeh domain were ramped along this fault and Hormuz salt was thickened in this process. The amount of uplift decreased along strike toward the Lorestan and Kazerun–Mangarak domains (Figs 1 and 2). Most of this advancing front is covered by the molasse sediments coming from the north.

Strike-slip faults

Differential propagation of the deformation front in the models led to formation of four dominant deflection zones offsetting the deformation front (Fig. 4). These deflection zones are transpressional and show a general trend parallel to the initial boundary between the viscous and frictional décollements (compare Figs 3 and 4). Some of these deflection zones are left-lateral and others are right-lateral strike-slip fault zones along which the deformation front was segmented and offset laterally a few centimetres in

the model (Fig. 4). Such deflection zones have been reported from analogue models by Cotton & Koyi (2000), who modelled the Salt Range and Potwar plateau of Pakistan.

In the Zagros fold and thrust belt, some strike-slip faults, for example the Kazerun Fault and the Bala Rud Fault (Fig. 1), have been described by Falcon (1974), Haynes & McQuillan (1974), Berberian (1995), Motiei (1995) and Talbot & Alavi (1996). These faults are generally attributed to reactivated basement faults. Below, we use model results to argue that even if some of these faults are basement related, their surface expression is amplified by the differential propagation of the deformation front above different décollements.

In map view, the Mountain Front Fault is offset by at least 160 km by the Kazerun Fault and 130 km along the Bala Rud Fault (Fig. 1; Berberian 1995; Hessami *et al*. 2001). However, the observed offset of the Mountain Front Fault along the Bala Rud and the Kazerun Faults may not be entirely caused by the strike-slip movement along basement faults. Our model results suggest that further propagation of deformation front in domain C, which simulates the Kazerun–Mangarak domain, could have given rise to right-lateral slip across the Mountain Front Fault (compare Figs 1 and 4). Thus, some of the surface offset along the Kazerun Fault must have originated from differential propagation of the deformation front in the sedimentary cover rather than being entirely caused by a reactivating basement fault. This inference suggests that even if the Kazerun Fault were absent or inactive in the basement, a significant amount of offset would have occurred as a result of differential propagation of the deformation front above the different décollements on either side of the fault.

The Bala Rud Fault west of the Dezful embayment trends east–west and offsets the Mountain Front Fault about 130 km (Fig. 1). This offset amount is measured in map view and there are no subsurface data across the fault. In addition, there are no well-known basement faults with the same trend in the Arabian platform to support the east–west-trending Arabian basement structural fabrics. The Bala Rud Fault has been defined as a basement fault by some previous workers (e.g. Motiei 1995; Hessami *et al*. 2001). However, based on model results and the lack of subsurface data for this fault, we present an alternative for its nature. Our models show that, as a result of differential propagation, there is an offset along the deflection zone at the boundary between domains A and B, which simulate the Lorestan and the Izeh domains, respectively. Therefore, we suggest that a considerable amount of movement along this strike-slip fault may have formed in the sedimentary cover as a result of differential propagation of the deformation front since late Cretaceous time (Fig. 2).

Motiei (1995) showed a left-lateral sense of displacement for the Nazamabad strike-slip fault between the Kazerun–Mangarak and Fars domains. In our model, significant deflection formed between domains C and D simulating these two domains, respectively. Model results suggest also that the Razak fault can be a right-lateral strike-slip fault. Similar to our models, the deformation front in the Fars platform is segmented and displaced by deflection zones about 50–60 km along this fault (compare Figs 1, 2 and 4)

Deformation pattern around the transpressional zones

Difference in rate of propagation of the deformation front between domains A and B led to the formation of a non-linear deformation front from the early stage of the shortening. Further shortening amplified curvatures in the deformation front and resulted in formation of deflection zones across the model. Thickening of the viscous substrate and the overburden behind the initial frontal ramp (see Fig. 3) led to development and subsequent amplification of the structural relief across the frontal ramp fault, especially in domain B, perpendicular to the shortening direction (Figs 3 and 7). This frontal fault was later offset by the deflection zones (Fig. 4). These deflection zones acted as lateral ramps. Above these lateral ramps, the traces of faults and folds form a low angle with the shortening direction (Fig. 4).

Similar features are seen in the Zagros fold and thrust belt, where there are some well-known folds (e.g. the Kaseh Mast, Kabood, Ghaleh–Nar and Lab–Seifid anticlines) whose trend is subparallel to the east–west-trending Bala Rud Fault in the western side of the Dezful embayment, whereas these folds are subparallel to the north–south-trending Kazerun Fault in the eastern side of the Dezful embayment (Motiei 1995; Sepehr 2001). These folds are truncated and dragged by the Bala Rud and Kazerun Faults. Subsurface evidence from drilling shows that these folds were fractured intensively by small-scale faults and closely spaced joints (Motiei 1995). Folds, which show an en echelon pattern in map view, appear to have been rotated progressively from a general NW–SE Zagros trend to make lower angles with the NE–SW-trending shortening. We do not have enough data to see whether such folds change in geometry or rotate. However, folds in the models tighten as they rotate along domain boundaries. Four small folds have east–west orientation along the Bala Rud Fault, which in association with the Mangarak Fault (the Kareh Bas Fault of Berberian 1995) show an anastomosing pattern. Talbot & Alavi (1996) suggested that these faults acted as a lateral footwall ramp, which transferred the NE–SW shortening between two different parts across the Zagros fold and thrust belt.

In comparison with the Bala Rud and the Kazerun Faults, the other strike-slip faults bounding the Fars platform are not very clear. They are apparently shorter and have smaller displacements (Motiei 1995). These faults were mapped from aerial photographs and satellite images by National Iranian Oil Company (1975) and Barzegar (1994).

Curvature of the deformation front

In our model, three arcs were developed along the deformation front. These are ‘antitaxial bends’ (Marshak 1988) so that their centre points moved further in the direction of transportation. The arcuate deformation front in domains C and E implies that the displacement changes gradually not abruptly above the lateral ramps. In our examples, the backstop was linear and there were no lateral changes in the amount of linear displacement. Therefore, we attribute the formation of arc shapes in the model to differential propagation of the deformation front above two different types of décollement. Comparison of initial widths (8 cm) of domains B and D (along strike of the domains) with those in plan view after 30% of shortening (5–6 cm) indicate that these domains narrowed with progressive shortening (Fig. 3). Applying this logic to the Zagros fold and thrust belt, it is suggested here that the Dezful embayment and the Fars platform may have started wider than their present width.

In the Zagros fold and thrust belt, there is no evidence for an irregular geometry of the backstop (Iranian plateau). The Main Zagros Reverse Fault, which is proposed to be the Zagros suture line, has approximately a straight trace (Figs 1 and 2). We therefore attribute the development of bends in the deformation front mainly to irregular initial distribution of the Hormuz salt. However, as deformation is thick-skinned in the Zagros, the

basement must also have contributed to the development of this geometry. During shortening, the domains underlain by a frictional décollement were pinned at this facies boundary. In contrast, the domains that were underlain by Hormuz salt were not pinned and could advance further.

The presence of the buttress in domains B and D resulted in reorientation of the deformation path along the model. This may explain why the deformation zone narrowed toward the lateral ramps in domains B and D. A map of particle path (Fig. 10) shows that material moves unevenly between the domains. In domains shortened above a viscous décollement (e.g. C and E) particle-path vectors diverge, whereas in domains shortened above a frictional décollement (e.g. B and D) the vectors converge. This explains why domains C and E have broadened along strike at the expense of domains B and D.

Our model results emphasize that the arcuate shapes and deflection zones along a young orogenic belt, such the Zagros fold and thrust belt, can be formed by initial variation in the mechanical characteristics of the décollement underlying the shortened cover units, rather than only by the reactivation of basement structures.

Conclusions

Model results suggest that structural evolution of a fold–thrust belt in which the sedimentary cover is shortened above décollements with different mechanical characteristics is governed by the configuration of the décollement. Spatial variation in the basal décollements can result in variation in deformation style and strain partitioning, wedge taper, and amount of sedimentation. Uneven distribution of a viscous substrate leads to an irregular deformation front comprising frontal and lateral ramps, and causes variations in the propagation rate of the deformation front and deformation zone width.

Model results demonstrate that some of the strike-slip faults and the Mountain Front Fault in the Zagros fold and thrust belt can be confined within structure offsetting the sedimentary cover only, rather than being deeper structures in the basement. Concentration of the thickest sedimentary sequence of the Zagros fold and thrust belt in the Dezful embayment, with the associated huge amount of hydrocarbon pools, can be attributed to a relatively high subsidence of a foreland in front of the Mountain Front Fault.

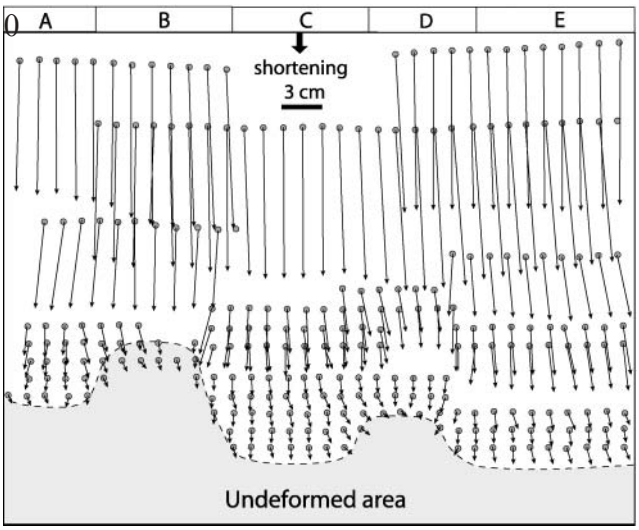

Fig. 10. Final particle-path map of the model, showing the amount of movement of passive markers during shortening of the model. It should be noted that the paths' vectors diverge in domains C and D, shortened above a viscous décollement and converge in domains B and D, shortened partly above a frictional décollement.

We thank G. I. Alsop and B. C. Vendeville for their thorough review and constructive comments on the manuscript. A. Skelton and C. J. Talbot are thanked for commenting on an earlier version of the manuscript. A.B. acknowledges a PhD grant from Uppsala University. H.A.K. is funded by the Swedish Research Council (VR).

Appendix: Scaling of models

To simulate any natural deformation by analogue modelling, models should be scaled using the principles of physical similarity described by, for example, Hubbert (1937) and Ramberg (1967). A scaled model should be similar to its prototype in geometry, kinematics and dynamics. For geometric similarity, we used a length ratio of 2.5×10^{-5} for vertical dimension implying that 1 cm in the models simulates 4 km in nature. However, a length ratio of 10^{-6} for horizontal dimension was used to calculate the lateral dimension (e.g. extent of the viscous layer simulating Hormuz salt). Consequently, the lengths and widths of different domains in the Zagros belt were calculated using this ratio. Different estimates for the thickness of the sedimentary cover in the Zagros fold and thrust belt and Hormuz salt have been given from different places along the belt (e.g. O'Brien 1957; James & Wynd 1965; Stöcklin 1968a; Player 1969; Falcon 1974; National Iranian Oil Company 1975; Berberian 1976,Berberian & Tchalenko 1976; Colman-Sadd 1978; Kent 1979, 1987; Murris 1980; Berberian & King 1981; Jackson & Fitch 1981; Jackson & McKenzie 1984; Snyder & Barazangi 1986; Beydoun 1991; Edgell 1991, 1996; Motiei 1993; Alavi 1994; Talbot & Alavi 1996; Sepehr 2001). These estimates range between 5 and 20 km. For the Hormuz salt, the estimated thickness varies between 0.9 and 4 km. Such variation in thickness of the sedimentary cover within different parts in the Zagros fold and thrust belt was not simulated in our model. Therefore the models are not scaled geometrically to the whole belt in thicknesses and heights, and may not be a strict replica of the Zagros fold and thrust belt. Although these models are not strictly dynamically scaled to the Zagros fold and thrust belt, the belt is used as a general guide. We use some parameters from the Zagros belt, but conduct preliminary calculations of timing of deformation in a prototype.

Suturing between the Iranian and Arabian plates led to shortening of the Zagros fold and thrust belt from NE to SW. In the models a one-end force simulating compression from the Iranian plate was used to approach qualitatively kinematic similarity. This means that a prototype, for example, the Zagros fold and thrust belt, would undergo a similar deformation history to that of the model.

Our choice of SGM-36 to simulate the Hormuz salt and loose sand for the frictional cover of Phanerozoic sediments leads to a dynamic similarity between the models and nature as explained below.

For the Newtonian behaviour of the transparent SGM-36 silicone, the following equation (see Price & Cosgrove 1990; Weijermars 1997) expresses the linear relationship between stress and strain rate:

$$\tau_v = \eta(v/h_v) = \eta\gamma_v \quad \text{(A1)}$$

where τ_v is the shear stress of the viscous layer, η is viscosity, υ is the velocity of the backstop, h_v is the thickness of the viscous layer and γ_v is the engineering shear strain rate assumed to be equal to the model strain rate (ε_m). This rate is calculated as the ratio between the thickness of the viscous layer and the velocity of the backstop (Weijermars 1997). Equation (A1) implies that the viscous layer behaves as a Newtonian material under strain rate lower than $\varepsilon_m = 3 \times 10^{-3}s^{-1}$ (see Weijermars 1986). By considering the thickness of the viscous layer (0.5 cm) and velocity of the backstop (3.2×10^{-4} cm s^{-1}), the model strain rate can be calculated as $\varepsilon_m = 6.4 \times 10^{-4}s^{-1}$.

To achieve dynamic similarity between the models and nature using a viscous layer, the Ramberg number (R) representing the ratio between gravity and viscous forces in model and nature (Weijermars & Schmeling 1986) must be equal. The Ramberg number in the model is

$$R_m = \rho_{vm} g h_{vm} / \eta_{vm} \varepsilon_m \quad (A2)$$

where $\rho_{vm} = 987 kgm^{-3}$ and $\eta_{vm} = 5 \times 10^4 Pas$, which are density and viscosity of the viscous layer (SGM-36) respectively, gravity acceleration $g = 9.87 ms^{-2}$, and strain rate $\epsilon_m = 6.4 \times 10^{-4}s^{-1}$. The Ramberg number is 1.52 in the models.

Following the same procedure, we calculate the Ramberg number for the prototype, using the Zagros fold and thrust belt as a general guide, where the thickness of Hormuz salt is assumed to be 2000 m

$$\eta_{vp} = \rho_{vp} g h_{vp} / R_p \varepsilon_p \quad (A3)$$

where $\rho_{vp} = 2200$ kg m^3 (Jackson *et al*. 1990) and $h_{vp} =$ 2000m are density and thickness of Hormuz salt. Viscosity of a typical salt is 10^{18}–10^{19} Pa s (Carter & Heard 1970; Lerche & O'Brien 1987). The viscosity of the Hormuz salt in the Zagros fold and thrust belt has been estimated to be as low as 10^{15}–10^{17} Pa s (Jackson *et al*. 1990; Weijermars *et al*. 1993). However, because of this high range in the estimates, we chose a 'safe' average of 10^{18} Pa s.

The horizontal velocity across the Zagros fold and thrust belt, reported recently by GPS measurements, is 11 mm a^{-1} for east of the Kazerun Fault (Hessami 2002). Although, this figure may not have been constant during deformation of the Zagros fold and thrust belt, we have used this figure to calculate the strain rate of the Zagros fold and thrust belt, $\epsilon_p = 1.74 \times 10^{-13}s^{-1}$. Using these values in equation (A3), the Ramberg number in nature is 24.38, which is only one order of magnitude higher than that calculated for the models, suggesting dynamic similarity with a prototype having the parameters used in the calculations.

Dry sand, which obeys the Coulomb–Mohr criterion of failure, was used to simulate the rheological behaviour of frictional cover. The Coulomb–Mohr criterion is defined as

$$\tau = C_o + \sigma\mu \quad (A4)$$

where τ and σ are shear and normal stresses, C_o is cohesive strength, and $\mu = \tan(\varphi)$ is the coefficient of internal friction, with φ being the angle of internal friction of a faulted material. For sediments in the upper crust, the angle of internal friction ranges between 31° and 40°, which gives a coefficient of internal friction ranging between 0.6 and 0.84 (Brace & Kohlstedt 1980; Krantz 1991). The cohesive strength of most rocks in the upper crust (C_o) is about 50 MPa (Byerlee 1978; Cobbold *et al*. 1989; Gaullier *et al*. 1993; Weijermars *et al*. 1993; Merle & Vendeville 1995). Loose sand with an internal frictional angle, $\varphi_m = 36°$ (coefficient of internal friction $\mu_m = 0.73$) (Krantz 1991; Cotton & Koyi 2000) and negligible cohesive strength is a suitable Coulomb–Mohr material for simulating the frictional behaviour of sedimentary cover.

To scale the models dynamically, the τ/σ ratio in model and nature should be equal (see Mulugeta 1988; Koyi *et al*. 1993; Weijermars *et al*. 1993; Childs *et al*. 1995):

$$(\tau/\sigma)_m = (\tau/\sigma)_p \quad (A5)$$

where subscripts m and p denote model and prototype.

As the normal stress σ can be defined as $\sigma = \rho g l$, where ρ is density, g is gravitational acceleration and l is length, equation (A5) can be rewritten as

$$(C_o/\rho g l)_m = (C_o/\rho g l)_p. \quad (A6)$$

The calculated τ/σ ratios, which were 1.8×10^{-1} and 7.1×10^{-1} for models and nature respectively, show acceptable approximation dynamic similarity between the model and the prototype fulfilling the geometric similarity.

Below, we use scaling parameters to calculate the time duration in the prototype. The time ratio T_r between prototype (T_p) and model (T_m) is defined by (e.g. Hubbert 1937; Ramberg 1967)

$$T_r = T_m/T_p = \varepsilon_p/\varepsilon_m = h_v \varepsilon_p/\nu. \quad (A7)$$

The $\varepsilon_p/\varepsilon_m$ ratio can be calculated using the strain rate of the model ($\varepsilon_m = 6.4 \times 10^{-4}s^{-1}$) and the prototype strain ratio (ε_p). If we use natural parameters of the Zagros fold and thrust belt, which is a general guide, the strain-rate ratio between the model and its prototype will be $\varepsilon_p/\varepsilon_m = 2.78 \times 10^{-10}$. Using equation (A7), the time ratio $T_r = 2.78 \times 10^{-10}$, then $T_p = 2.06 \times 10^{14}$s or 6.5 Ma (late Miocene). Surprising, this time duration fits well with the time of deformation in the Zagros fold and thrust belt (O'Brien 1957; Stöcklin 1968*b*; Falcon 1974; Colman-Sadd 1978; Kent 1979; Murris 1980; Berberian & King 1981; Hempton 1987; Ameen 1991; Talebian & Jackson 2002).

References

Alavi, M. 1994. Tectonics of the Zagros Orogenic belt of Iran: new data and interpretations. *Tectonophysics*, **229**, 211–238.

Ameen, M.S. 1991. Alpine geowarpings in the Zagros–Taurus range: influence on hydrocarbon migration and accumulations. *Journal of Petroleum Geology*, **14**, 417–428.

Baker, C., Jackson, J. & Priestly, K. 1993. Earthquakes on the Kazerun line in the Zagros mountains of Iran, strike-slip faulting within a fold and thrust belt. *Geophysical Journal International*, **115**, 41–61.

Barzegar, F. 1994. Basement fault mapping of E Zagros folded belt (S.W. Iran) based on space-borne remotely sensed data. *Proceedings of the 10th Thematic Conference on Geologic Remote Sensing: Exploration, Environment, and Engineering*. Environmental Research Institute of Michigan, MI, 455–466.

Berberian, M. 1995. Master 'blind' thrust faults hidden under the Zagros folds: active tectonics and surface morphotectonics. *Tectonophysics*, **241**, 193–224.

Berberian, M. & King, G.C.P. 1981. Towards a paleogeography and tectonic evolution of Iran. *Canadian Journal of Earth Sciences*, **18**, 210–265.

Berberian, M. & Tchalenko, J. 1976. *Earthquakes of Bandar Abbas–Hajiabad Region (Zagros, Iran)*. Geological Survey of Iran, Report, **39**, 371–396.

Beydoun, Z.R. 1991. *Arabian Plate Hydrocarbon Geology and Potential—a Plate Tectonic Approach*. American Association of Petroleum Geologists, Studies in Geology, **33**.

Beydoun, Z.R., Hughes, M.W. & Stoneley, R. 1992. Petroleum in the Zagros basin: a late Tertiary foreland basin overprinted onto the outer edge of the vast hydrocarbon-rich Paleozoic–Mesozoic passive margin shelf. *In:* Macqueen, R.W. & Leckie, D.A. (eds) *Fureland Basins and Fold Belts*. American Association of Petroleum Geologists, Memoirs, **55**, 307–336.

Bonini, M. 2001. Passive roof thrusting and forelandward fold propagation in scaled brittle–ductile physical models of thrust wedges. *Journal of Geophysical Research*, **106**, 2291–2311.

Brace, W.F. & Kohlstedt, D.L. 1980. Limits on lithosphere stress imposed by laboratory experiments. *Journal of Geophysical Research*, **85**, 6248–6252.

Butler, R.W., Coward, M.P., Harwood, G.M. & Knipe, R.J. 1987. Salt control

on thrust geometry, structural style and gravitational collapse along the Himalayan mountain front in the Salt Range of northern Pakistan. *In:* Lerche, I. & O'Brien, J.J. (eds) *Dynamical Geology of Salt and Related Structures*. Academic Press, New York, 339–418.

Byerlee, J. 1978. Friction of rocks. *Pure and Applied Geophysics*, **116**, 615–625.

Carter, N.J. & Hansen, F.D. 1983. Creep of rocksalt. *Tectonophysics*, **92**, 275–333.

Carter, N.L. & Heard, H.C. 1970. Temperature and rate dependent deformation of halite. *American Journal of Science*, **269**, 193–249.

Chapple, W.M. 1978. Mechanics of a thin-skinned fold-and-thrust belt. *Geological Society of American Bulletin*, **89**, 1189–1198.

Childs, C., Watterson, J. & Walsh, J.J. 1995. Fault overlap zones within developing normal fault systems. *Journal of the Geological Society, London*, **152**, 535–549.

Cobbold, P.R., Rossello, E.A. & Vendeville, B. 1989. Some experiments on interacting sedimentation and deformation above salt horizons. *Bulletin de la Société Géologique de France*, **8**, 453–460.

Colman-Sadd, S.P. 1978. Fold development in Zagros simply folded belts, southwest Iran. *AAPG Bulletin*, **62**, 984–1003.

Costa, E. & Vendeville, B.B. 2002. Experimental insights on the geometry and kinematics of fold-and-thrust belt above weak, viscous evaporitic décollement. *Journal of Structural Geology*, **24**, 1729–1739.

Cotton, J.T. & Koyi, H.A. 2000. Modelling of thrust fronts above ductile and frictional décollements: application to structures in the Salt Range and Potwar Plateau, Pakistan. *Geological Society of America Bulletin*, **112**, 351–363.

Davis, D.M. & Engelder, T. 1985. The role of salt in fold-and-thrust belts. *Tectonophysics*, **119**, 67–88.

Davis, D.M. & Engelder, T. 1987. Thin-skinned deformation over salt. *In:* Lerche, I. & O'Brien, J.J. (eds) *Dynamical Geology of Salt and Related Structures*. Academic Press, New York, 301–337.

Davy, P. & Cobbold, P.R. 1991. Experiments on shortening of 4-layer model of continental lithosphere. *Tectonophysics*, **188**, 1–25.

Dixon, J.M. & Liu, S. 1992. Centrifuge modelling of the propagation of thrust faults. *In:* McClay, R.R. (ed.) *Thrust Tectonics*. Chapman and Hall, London, 53–69.

Edgell, H.S. 1991. Proterozoic salt basins of the Persian Gulf area and their role in hydrocarbon generation. *Precambrian Research*, **54**, 1–14.

Edgell, H.S. 1996. Salt tectonics in the Persian Gulf basin. *In:* Alsop, G.L., Blundell, D.L. & Davison, I. (eds) *Salt Tectonics*. Geological Society, London, Special Publications, **100**, 129–151.

Falcon, N.L. 1961. Major earth-flexing in the Zagros Mountains of southwest Iran. *Quarterly Journal of the Geological Society, London*, **117**, 367–376.

Falcon, N.L. 1967. The geology of the north-east margin of the Arabian basement shield. *Advancement of Science*, **24**, 1–12.

Falcon, N.L. 1974. South Iran: Zagros Mountains. *In:* Spencer, A.M. (ed.) *Mesozoic–Cenozoic Orogenic Belts—Data for Orogenic Studies*. Geological Society, London, Special Publications, **4**, 199–211.

Gaullier, V., Brun, J.P., Guerin, G. & Leconu, H. 1993. Raft tectonics: the effects of residual topography below a salt décollement. *Tectonophysics*, **228**, 363–381.

Haynes, S.J. & McQuillan, H. 1974. Evaluation of the Zagros suture zone, Southern Iran. *Geological Society of American Bulletin*, **85**, 739–744.

Hempton, M.R. 1987. Constraints on Arabian plate motion and extensional history of the Red Sea. *Tectonics*, **6**, 687–705.

Hessami, K. 2002. *Tectonic history and present-day deformation in the Zagros fold–thrust belt*. PhD thesis, Uppsala University.

Hessami, K., Koyi, H.A. & Talbot, C.J. 2001. The significance of strike slip faulting in the basement of the Zagros fold–thrust belt. *Journal of Petroleum Geology*, **24**, 5–28.

Hubbert, M.K. 1937. Theory of scale models as applied to geologic structures. *Geological Society of America Bulletin*, **48**, 1459–1520.

Husseini, M.I. 1988. The Arabian Infracambrian extensional system. *Tectonophysics*, **148**, 93–103.

Jackson, J.A. 1980. Reactivation of basement faults and crustal shortening in orogenic belts. *Nature*, **283**, 343–346.

Jackson, J.A. & Fitch, T.J. 1981. Basement faulting and focal depths of the larger earthquakes in the Zagros mountains (Iran). *Geophysical Journal of the Royal Astronomical Society*, **64**, 561–586.

Jackson, J.A. & McKenzie, D.P. 1984. Active tectonics of Alpine–Himalayan belt between western Turkey and Pakistan. *Geophysical Journal of the Royal Astronomical Society*, **77**, 185–264.

Jackson, J.A., Fitch, T.J. & McKenzie, D.P. 1981. Active thrusting and evolution of the Zagros fold belt. *In:* McClay, K. & Price, N.J. (eds) *Thrust and Nappe Tectonics*. Geological Society, London, Special Publications, **9**, 371–379.

Jackson, J.A., Haines, J. & Holt, W. 1995. The accommodation of Arabian–Eurasia plate convergence in Iran. *Journal of Geophysical Research*, **100**, 15205–15219.

Jackson, M.A.P. & Talbot, C.J. 1986. External shapes, strain rates, and dynamics of salt structures. *Geological Society of America Bulletin*, **97**, 305–323.

Jackson, M.P.A., Cornelius, R.R., Craig, C.H., Gansser, A., Stöcklin, J. & Talbot, C.J. 1990. *Salt Daipirs of the Great Kavir, Central Iran*. Geological Society of America, Memoirs, **177**.

James, G.A. & Wynd, J.G. 1965. Stratigraphical nomenclature of Iranian Oil Consortium Agreement Area. *AAPG Bulletin*, **49**, 2182–2245.

Kent, P.E. 1958. Recent studies of south Persian salt plugs. *AAPG Bulletin*, **42**, 2951–2972.

Kent, P.E. 1979. The emergent Hormuz salt plugs of southern Iran. *Journal of Petroleum Geology*, **2**, 117–144.

Kent, P.E. 1987. Island salt plugs in the Middle East and their tectonic implications. *In:* Lerche, I. & O'Brien, J.J. (eds) *Dynamical Geology of Salt and Related Structures*. Academic Press, New York, 3–38.

Koyi, H. 1988. Experimental modeling of role of gravity and lateral shortening in Zagros mountain belt. *AAPG Bulletin*, **72**, 1381–1394.

Koyi, A.H., Jenyon, M.K. & Petersen, K. 1993. The effect of basement faulting on diapirism. *Journal of Petroleum Geology*, **16**, 285–312.

Koyi, H.A., Hessami, K. & Teixell, A. 2000. Epicenter distribution and magnitude of earthquakes in fold–thrust belts: insights from sandbox models. *Geophysical Research letters*, **27**, 273–276.

Krantz, R.W. 1991. Measurements of friction coefficients and cohesion for faulting and fault reactivation in laboratory models using sand and sand mixtures. *Tectonophysics*, **188**, 203–207.

Lerche, I. & O'Brien, J.J. 1987. Modelling of buoyant salt diapirism. *In:* Lerche, I. & O'Brien, J.J. (eds) *Dynamical Geology of Salt and Related Structures*. Academic Press, New York, 129–162.

Letouzey, J., Colletta, B., Vially, R. & Chermette, J.C. 1995. Evolution of salt-related structures in compressional settings. *In:* Jackson, M.P.A., Roberts, D.G. & Snelson, S. (eds) *Salt Tectonics. A Global Perspective*. American Association of Petroleum Geologists, Memoirs, **65**, 41–60.

Liu, Huiqi, McClay, K.R. & Powell, D. 1992. Physical models of thrust wedges. *In:* McClay, K.R. (ed.) *Thrust Tectonics*. Chapman and Hall, London, 71–81.

Marshak, S. 1988. Kinematics of orocline and arc formation in thin-skinned orogens. *Tectonics*, **7**, 73–86.

Marshak, S., Wilkerson, M.S. & Hsui, A.T. 1992. Generation of curved fold–thrust belt: insight from simple and analytical models. *In:* McClay, K.R. (ed.) *Thrust Tectonics*. Chapman and Hall, London, 83–92.

Merle, O. & Vendeville, B. 1995. Experimental modelling of thin-skinned shortening around magmatic intrusions. *Bulletin of Volcanology*, **57**, 33–43.

Motiei, M. 1993. *Stratigraphy of Zagros*. Geological Survey of Iran, Tehran (in Farsi).

Motiei, H. 1995. *Petroleum Geology of Zagros*. Geological Survey of Iran, Tehran (in Farsi).

Mulugeta, G. 1988. Modelling the geometry of coulomb thrust wedges. *Journal of Structural Geology*, **10**, 847–859.

Murris, R.J. 1980. Middle East: stratigraphic evolution and oil habitat. *AAPG Bulletin*, **64**, 597–618.

National Iranian Oil Company 1975. *Tectonic Map of Iran*. National Iranian Oil Company, Exploration and Production, Tehran.

Ni, J. & Barazangi, M. 1986. Seismotectonics of the Zagros continental collision zone and a comparison with the Himalayas. *Journal of Geophysical Research*, **9**, 8205–8218.

O'Brien, C.A.E. 1957. Salt diapirism in South Persia. *Geologie en Mijnbouw*, **19**, 337–376.

Player, R.A., 1969. *The Hormuz salt plugs of southern Iran*. PhD thesis, Reading University.

Price, N.J. & Cosgrove, J.W. 1990. *Analysis of Geological Structures*. Cambridge University Press, Cambridge.

Ramberg, H. 1967. *Gravity Deformation and the Earth's Crust*, *1st*. Academic Press, London.

Ricou, L.E., Braud, J. & Brunn, J.H. 1977. Le Zagros. *Mémoire Hors Série, Société Géologique de France*, **8**, 33–52.

Scott, B. 1981. The Eurasian–Arabian and African continental margin from Iran to Greece. *Journal of the Geological Society, London*, **138**, 719–733.

Sengör, A.M.C. & Kidd, W.S.F. 1979. Post-collisional tectonics of the Turkish–Iranian plateau and a comparison with Tibet. *Tectonophysics*, **55**, 361–376.

Sepehr, M., 2001. *The tectonic significance of the Kazerun fault zone, Zagros fold–thrust belt, Iran*. PhD thesis, Imperial College, London.

Snyder, D.B. & Barazangi, M. 1986. Deep crustal structural and flexure of the Arabian plate beneath Zagros collisional mountain belt as inferred from gravity observation. *Tectonophysics*, **5**, 361–373.

Spaargaren, F.A. 1987. *Geological Map of Iraq and South-western Iran*. Robertson Research Publications, Llandudno.

Stöcklin, J. 1968*a*. Salt deposits of the Middle East. *In:* Mattox, R.B. (ed.) *Saline Deposits: a Symposium based on Papers from the International Conference on Saline Deposits, Houston, Texas, 1962*. Geological Society of America, Special Papers, **88**, 157–181.

Stöcklin, J. 1968*b*. Structural history and tectonics of Iran: a review. *AAPG Bulletin*, **52**, 1229–1258.

Stoneley, R. 1981. The geology of the Kuh-e-Dalneshin area of southern Iran and its bearing on the evaluation of Southern Tethys. *Journal of the Geological Society, London*, **138**, 509–526.

Talbot, C.J. 1992. Centrifuge models of Gulf of Mexico profiles. *Marine and Petroleum Geology*, **9**, 412–432.

Talbot, C.J. & Alavi, M. 1996. Salt Tectonics. *In:* Alsop, G.I., Blundell, D.J. & Davison, I. (eds) Geological Society, London, Special Publications, **100**, 89–109.

Talebian, M. & Jackson, J. 2002. Offset on the Main Recent Fault of NW Iran and implications for late Cenozoic tectonics of the Arabia–Eurasia collision zone. *Geophysical Journal International*, **150**, 422–439.

Urai, J.L., Spiers, C.J., Zwart, H.J. & Lister, G.S. 1986. Weakening of rock salt by water during long-term creep. *Nature*, **324**, 554–557.

Velaj, T., Davison, I., Serjani, A. & Alsop, A. 1999. Thrust tectonics and the role of evaporites in the Ionian Zone of the Albanides. *AAPG Bulletin*, **83**, 1408–1425.

Vita Finzi, C. 1978. ^{14}C deformation chronologies in coastal Iran, Greece, Jordan. *Journal of the Geological Society, London*, **144**, 553–560.

Vita Finzi, C. 2001. Neotectonics at the Arabian plate margins. *Journal of Structural Geology*, **23**, 521–530.

Weijermars, R. 1986. Flow behaviour and physical chemistry of Bouncing Putties and related polymers in view of tectonics laboratory applications. *Tectonophysics*, **124**, 325–358.

Weijermars, R. 1997. Flow behaviour and physical chemistry of bouncing putties and related polymers in view of tectonic laboratory application. *Tectonophysics*, **124**, 325–358.

Weijermars, R. & Schmeling, H. 1986. Scaling of Newtonian and non-Newtonian fluid dynamics without inertia for quantitative modelling of rock flow due to gravity (including the concept of rheological similarity). *Physics of the Earth and Planetary Interiors*, **43**, 316–330.

Weijermars, R., Jackson, M.P.A. & Vedeville, B.C. 1993. Rheological and tectonic modelling of salt provinces. *Tectonophysics*, **217**, 143–174.

Received 21 October 2002; revised typescript accepted 25 February 2003.
Scientific editing by Alex Maltman